Simulation of a quantum particle using NMR

A thesis submitted towards partial fulfilment of
BS-MS Dual Degree Programme

by

Ravi Shankar

under the guidance of

Dr. T. S. Mahesh

Assistant Professor, IISER Pune

Indian Institute of Science Education and Research
Pune

Certificate

This is to certify that this thesis entitled *Simulation of a quantum particle using NMR* submitted towards the partial fulfilment of the BS-MS dual degree programme at the Indian Institute of Science Education and Research Pune represents original research carried out by **Ravi Shankar** at Indian Institute of Science Education and Research Pune, under the supervision of **Dr T. S. Mahesh** during the academic year 2012-2013.

Ravi Shankar
(Student)

T. S. Mahesh
(Supervisor)

Acknowledgements

I consider myself lucky to have got Mahesh sir as my mentor. He's very approachable, entertains even the silliest of ideas and goes quite easy on you when you screw things up - oh yes, I have! He's very understanding too - greets you with a smile even when you bunk off lab for a couple of days and return.

I'm thankful to - Swathi for helping me with the experiments and for being available even on weekends to toil in freezing conditions; - Hemant and Kota for I have essentially used their GRAPE program for my simulations and also for the many entertaining conversations we have had; - Abhishek for being keeping me company in lab late at night many a time; - Bhargava and Nitesh for various productive and unproductive discussions. It would border on hypocrisy (only justifiably so) if I fail to thank Phillip Morris for coming up with a great stimulant. I'm also grateful to my dad for being so supportive and understanding of my ambitions.

I'm indebted to KVPY, DST for funding my high-life through all my years in IISER-P. Needless to say, I'm highly appreciative of all my friends who have always kept the fun quotient in my life sky-high.

Abstract

Classical computers require exponential time for simulating the dynamics of quantum systems. But computers built using the laws of quantum mechanics are expected to take way lesser time. Challenge has not just been in constructing one, but even in controlling quantum phenomena at an experimental level. Though a large scale quantum computer, based on conventional NMR, may never be built, NMR is considered to be an accessible test-bed for experimental quantum computing. We here simulate single particle Schrodinger equation for various potentials, effectively realising a NMR quantum simulator. Discretisation of space owing to limited number of qubits however limits the precision of the simulator. However the successful demonstration of Schrodinger evolution by a machine that is governed by quantum laws keeps one's quest for a quantum computer alive.

Contents

Chapter 1

Introduction

Computation and Communication in today's world are governed largely my laws of classical mechanics. A Quantum Computer taps into the potential now offered to us by the more fundamental laws of quantum mechanics.

Gordan Moore observed in 1965 that the number of components in integrated circuits (IC) had doubled every year since the invention of IC since 1958 and predicted the trend to continue for at least a decade [1]. Remarkably, Moore's law has held true for over fifty years now. The improvement in computer performance thus far has largely been due to the reduction in transistor size among other things. But this trend can not go on forever as quantum mechanical effects are bound get more pronounced and hinder transistor performance. Feynman in 1981 suggested that we use quantum effects to our advantage in building a computer - a quantum computer [2].

A major development that transformed quantum computing from being just a fancy idea to research interest of many is Shor's prime factorization algorithm [3] in 1995. The algorithm solves the classically intractable (requiring exponential time) problem of prime factorisation in polynomial time (tractable). Since then, there has been immense progress in theoretical quantum computation - unsorted database search algorithm [4], cryptography, teleportation[5], etc.

The most appealing feature of quantum computing is quantum parallelism - a phenomemon in which computing is done with more than one input *si-*

multaneously. A classical bit - the building block of classical computers - is either in state 0 or in state 1. But a qubit (quantum bit) can also exist in a coherent superposition of both 0 and 1. This property manifests as quantum parallelism with any operation on a set of qubits (or a register).

Computational power of computers are not as such limited by any physical law. However as irreversible computations are associated with loss of information (which corresponds to energy) and that there is a thermodynamic limit on how much heat a system can dissipate, a computer which is to perform arbitrarily fast must be built using reversible gates [6]. In this regard, quantum gates which simply transform a quantum system state from one point to a different in a Hilbert space can be described using unitary operators and are thus reversible.

NMR techniques are capable of initialising (pseudo) pure states and can implement logic gates. It also has relatively long decoherence times. All these make NMR techniques suitable for *small* quantum computers [7]. Progress in NMR computation has been immense with demonstrations of Deutsch's algorithm [8] Grover's search algorithm [9] and quantum counting [10] to name a few. Like any other quantum computing technology, NMR quantum computing also has some fundamental difficulties including its inability to perform projective measurements - read-out involves ensemble measurements and expectation values, and in scaling up the number of qubits [7]. Conventional NMR QIP experiments have not created genuine entanglement [11] and the pseudo pure states mentioned earlier are essentially mixed states that mimics a pure state in the context of the experiment and so, are not non-seperable, in general.

Even with all the limitations, NMR is a very good choice for small scale quantum computing problems including the simulation of Schrodinger equation - the subject of this thesis.

If ever there is to be a computer simulation of physics, that which involves strange phenomena that can only be explained by the laws of quantum mechanics, it can only be through a quantum computer. A classical computer simply cannot imitate quantum mechanics [2].

> *nature isn't classical, dammit, and if you want to make a simulation of nature, you'd better make it quantum mechanical.*
>
> - Richard Feynman

Simulation of single-particle Schrodinger equation, though does not involve any of the strange quantum mechanical phenomena that can't be imitated by a classical computer, is a challenging enough problem to implement on a quantum computer.

Chapter 2

Introduction to NMR

2.1 NMR Theory

Spin is a fundamental property of nature like charge or mass. NMR exploits the effects of nuclear spins. The angular momentum associated with nuclear spin is quantized. The z-component of angular momentum vector is given by $S_z = m\hbar$. Therefore the z-component of magnetic moment $\mu_z = \gamma S_z = \gamma m\hbar$. γ here is the gyromagnetic ratio of the nucleus. A spin-$\frac{1}{2}$ nucleus has two possible spin states: $m = \frac{1}{2}$ or $m = -\frac{1}{2}$. In the absence of any external field, these two states are degenerate. However in a magnetic field, the states split due to the interaction of the nuclear magnetic moment with the external magnetic field - Zeeman interaction.

$$H = -\vec{\mu}.\vec{B}_0$$

$E = -\mu.B_0$. Taking the magnetic field axis to be z-axis, $E = -\mu_z.B_0 = -\gamma m\hbar B_0$. This implies $\Delta E = \gamma\hbar B_0$. The spin state with lower energy has more population than the state with higher energy. Magnetic moments precess around the net magnetic field with larmor frequency[1], $\omega = \gamma B_0$. Nuclear spins exhibit resonant absorption only when the frequency of electromagnetic radiation matches the larmor frequency (which is usually in the

[1]The precession of magnetic moments of nuclei about an external magnetic field due to the torque on the moment by the field is referred to as Larmor precession. The precession rate, $\omega = -\gamma B$

radio frequency range). This nuclear magnetic resonant absorption is what is observed in NMR. It might seem that all nuclei of the same isotopic species would resonate at the same frequency. But it's not the case due to the shielding effect of the surrounding electrons which in general reduces the effective magnetic field present at the nucleus. Electrons also rotate with a spin to produce small magnetic fields opposite to the external magnetic field. This causes the effective magnetic field to reduce, in general. Therefore the energy gap between the spin states and the hence the larmor frequency reduce. The apparent shift in the larmor frequency is termed as *chemical shift*.

NMR hardware has RF coils in the transverse direction (XY plane) to create time-dependent magnetic field $B_1(t)$ in the transverse direction to rotate the net magnetisation in a pulse sequence. It is also used to detect the net transverse magnetisation.

2.1.1 Relaxation

At equilibrium, the net magnetization points along the direction of the applied magnetic field and the density matrix describing the state only has diagonal terms (state with no coherences). The process by which any other perturbed state returns to this equilibrium state, when left on its own for long enough, is termed *relaxation*.

T1 Relaxation

Also called as spin-lattice or longitudinal relaxation, T1 relaxation is a process by which M_z returns to its equilibrium value M_0. Nuclei precessing about the external magnetic field experience slightly different local magnetic field (both magnitude and direction) because of the surrounding magnetic electrons and nuclei. The thermal motion of the molecules makes the local magnetic field time-dependent is the prime cause that drives the spins to orient along the external magnetic field. T1 is defined as the decay constant (time) in such a recovery of M_z to M_0.

T2 Relaxation

Once off the z-axis, the difference in larmor frequencies of different nuclei come to play as spins start to precess about the z-axis at different rates.

The differences in larmor frequencies can be due to the time-dependent local magnetic field caused by thermal motion of molecules or due to inhomogeneity in the external magnetic field. Both result in dephasing of transverse magnetization with time. The former is irreversible due to the randomness in thermal motion and is called *decoherence* while the latter - *incoherence* - can be reversed by techniques such as Hahn echo T2 is defined to be the time constant for decay of transverse magnetisation to zero.

In general, T2 is less than or equal to T1.

2.1.2 Pulses

Transverse magnetic field B_1 which can be created using rf-coils is used to flip the net magnetic field about any axis on the XY-plane. The flip angle θ_p of a pulse p about an axis is given by $-\gamma B_p \tau_p$ where τ_p is the pulse time and B_p is the rf magnetic field amplitude. A π_x-pulse rotates the net magnetisation about X-axis by an angle of π radians.

2.1.3 Signal

On application of the detection pulse, $\frac{\pi}{2}_x$, magnetization is made to point along -y direction. Spins start to precess about the z axis. The rf-receiver measures the transverse magnetization, which decays with time, thus producing a signal which is termed *free induction decay* (FID). The fourier transform of FID, which is in time domain, gives us the spectrum in frequency domain.

In a single qubit system there are two possible spin states in the presence of an external magnetic field. The spin states precess about the z axis with same frequencies, only with opposite senses of direction. Owing to the bias in the population distribution which favours the lower energy state (which has magnetisation pointing along the external magnetic field), we get a single line in the spectrum corresponding to the larmor frequency of the lower energy state. The intensity of the line depends on the excess population of the lower state over the higher energy state. As the transition probability depends on the population difference betweent the two states, we can interpret the intensity as a measure of the transition probability too.

In case of a n-qubit system, a particular state of $n-1$ qubits is split into two

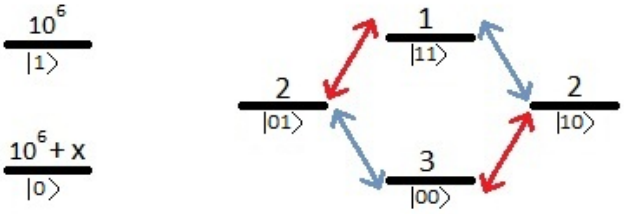

Figure 2.1:

by the other qubit. The population difference between the two states corresponds to a line in the spectrum. Thus we have $2^{(n-1)}$ lines corresponding to every qubit and in total, $n.2^{(n-1)}$ lines in the spectrum. The case of a two qubit system is illustrated in figure 2.1.

2.2 GRAPE

In NMR, one often needs to find optimal pulse sequences that guide a spin system ρ_0 in a specified time T to a density operator ρ_T that resembles a target operator C. Gradient Ascent Pulse Engineering (GRAPE)[12] is an algorithm that achieves it efficiently.

The equation of motion of a spin system state is given by the Liouville-von Neumann equation

$$\dot{\rho}(t) \;=\; -i\left[\left(H_0 + \sum_{k=1}^{m} u_k(t)H_k\right), \rho(t)\right] \tag{2.1}$$

H_0 here is the free evolution Hamiltonian and H_k correspond to rf-Hamiltonians (control fields) - which are basically evolution due to the transverse magnetic field B_1 created by the rf-coils.

$\langle C|\rho(t)\rangle = trace(C^\dagger \rho(t))$ gives a measure (ϕ) of the overlap between the spin system density operator and the target operator. The goal of GRAPE is to maximise C. The algorithm stems from the realisation that ϕ is improved

when we transform $u_k(j) \rightarrow u_k(j) + \epsilon \frac{\delta \phi}{\delta u_k(j)}$ where ϵ is a small step size. We iteratively perform the transformation until the change in ϕ is within a threshold. GRAPE is a relatively new method which is orders of magnitude faster than the conventional methods used in NMR.

Chapter 3

Dynamics of Quantum Systems

The dynamics of one-dimensional quantum systems are governed by the time-dependent Schrodinger equation,

$$i\hbar\frac{\partial\psi}{\partial t} = H\psi. \tag{3.1}$$

Unlike the classical mechanics, quantum mechanics paints a probabilistic world view, not a deterministic one. The wave function ψ when squared gives only the probability of detecting a particle at a position x at a time t. This limitation results neither from of our lack of knowledge nor from want of better technology. It is merely a manifestation of an unavoidable uncertainty about the position and time of events in the quantum realm.

The rule that the square of ψ gives the probability (and not cube or any other function of ψ), commonly referred to as Born's rule [13], is one of the fundamental laws of quantum mechanics. There have been many attempts to derive the rule from other assumptions of quantum mechanics, but all in vain. Though with the startling predictions of quantum mechanics being verified in various experiments validating the rule, there is still a doubt on its accuracy [14] [15]. A concrete evidence for the exactness of the rule is sought.

3.1 Schrodinger Equation

The Schrodinger equation for the evolution of a one-dimensional system in x-basis

$$i\hbar\frac{\partial\psi}{\partial t} = \frac{-\hbar^2}{2m}\frac{\partial^2\psi}{\partial x^2} + V\psi \tag{3.2}$$

has the solution

$$\psi(x, t+\epsilon) = e^{-\frac{i\widehat{H}\epsilon}{\hbar}}\psi(x,t) \tag{3.3}$$

where $\widehat{H} = H_0 + V$; $H_0 = -\frac{\hbar^2}{2m}\frac{d^2}{dx^2}$ and $V = V(x)$.
Clearly $e^{-\frac{iV\epsilon}{\hbar}}$ is diagonal. However the first term in the operator $\widehat{H}$ involves a double derivative with respect to x and so is not diagonal. This problem can be overcome if we transform the wavefunction into p-basis and solve for the H_0 term.

The Fourier transform in continuous space is given by

$$\widetilde{\psi}(k,t) = \frac{1}{\sqrt{2\pi}}\int_{-\infty}^{\infty}\psi(x,t)e^{-ikx}dx$$

and the associated inverse by

$$\psi(x,t) = \frac{1}{\sqrt{2\pi}}\int_{-\infty}^{\infty}\widetilde{\psi}(k,t)e^{ikx}dk$$

The time-dependent Schrodinger equation in p-basis thus becomes

$$i\hbar\frac{\partial\widetilde{\psi}}{\partial t} = \frac{\hbar^2k^2}{2m}\widetilde{\psi} + V(i\frac{\partial}{\partial k})\widetilde{\psi} \tag{3.4}$$

Clearly equations 3.2 and 3.4 provide us with one term each - potential and kinetic energy, respectively, for the evolved ψ.

$$\psi(x, t+\epsilon) = \psi(x,t)e^{-iV(x)\epsilon/\hbar}$$

$$\widetilde{\psi}(k, t+\epsilon) = \widetilde{\psi}(k,t)e^{-i\hbar k^2\epsilon/2m}$$

But to make use of the above mentioned method, we need to be able to split e^{H_0+V} into e^{H_0} and e^V. But simply splitting the term into two exponentials is not valid as $\widehat{H_0}$ and $\widehat{V}$ do not commute. However given ϵ to be sufficiently small, we may write

$$\psi(x, t+\epsilon) = e^{-\frac{iV\epsilon}{2\hbar}}e^{-\frac{iH_0\epsilon}{\hbar}}e^{-\frac{iV\epsilon}{2\hbar}} \qquad [1](\text{Trotter decomposition A.2}) \tag{3.5}$$

[1]In doing so, we have only ignored ϵ^3 and higher order terms.

3.2 Discretisation

To simulate the evolution of an one-dimensional system we, in NMR, use a very limited number of qubits. The finite number of states ($2^n; n =$ number of qubits) requires us to discretise spaces (both x and p, of course not seperately) in the problem[16]. Discretisation modifies Fourier transformation in the following manner.

$$\widetilde{\psi}(k,t) = \frac{1}{\sqrt{2\pi}} \int_a^b \psi(x,t) e^{-ikx} dx \tag{3.6}$$

Here the limit has been changed from $[-\inf, \inf]$ to $[a, b]$. This is a safe assumption provided our ψ is localised in the range $[a,\ b]$. [2]

To approximate the integral in 3.6 as a sum of N ($= 2^n$ terms) we define:

$$\Delta x = \tfrac{(b-a)}{N} \text{ which implies } x_n = x_0 + n\Delta x$$

$$\Delta k = \tfrac{2\pi}{N\Delta x} \text{ which implies } k_m = k_0 + m\Delta k$$

which make

$$\widetilde{\psi}(k,t) \simeq \frac{1}{\sqrt{2\pi}} \sum_{n=0}^{N-1} \psi(x_n,t) e^{-ikx_n} \Delta x \tag{3.7}$$

$$= \frac{1}{\sqrt{2\pi}} \Sigma_{n=0}^{N-1} \psi e^{-i\pi n} e^{\frac{2\pi i}{N} mn} \Delta x \qquad \text{(refer to A.1)} \tag{3.8}$$

The above equality follows from limiting the range of k to $[-\frac{\pi}{\Delta x}, \frac{\pi}{\Delta x}]$, which would imply that high frequency (momentum) terms are ignored. This is an unavoidable consequence of discretization, in accordance with Nyquist sampling theorem [3].

3.3 Algorithm

In brief, all we need to do to simulate the evolution of a one-dimensional quantum system is to construct three unitary matrices: $e^{-\frac{iV\delta t}{2\hbar}}$, $e^{-i\hbar k^2 \delta t/2m}$

[2] Equivalently one can assume that $V = \inf$ for $x < a$ and $x > b$

[3] Nyquist Sampling theorem: If a function has $\Delta x = B$, then the maximum frequency it can faithfully represent is $\frac{1}{2B}$.

and QFT (using the relation **??**), of sizes N$\times$ N each. We will also need Inverse QFT, which is simply $QFT^{\dagger}$.

Steps to evaluate $\psi(x,t)$:

1. Declare $\psi(x,0)$ in discrete points of x.
2. Evaluate $\psi(x,\delta t) = e^{-\frac{iV\delta t}{2\hbar}}.[\text{IQFT}].e^{-i\hbar k^2\delta t/2m}.[\text{QFT}].e^{-\frac{iV\delta t}{2\hbar}}\psi(x,0)$.
3. Repeat step (2) m times for further evolution of ψ until $m\delta t = t$.

One must choose the domain of ψ - Δx and δt - wisely. A large Δx limits k_{max} and thereby affects the simulation. δt must be small to ensure the validity of Trotter approximation being used.

A sample simuation of a gaussian wavepacket evolving in a linear potential is given in figure 3.3

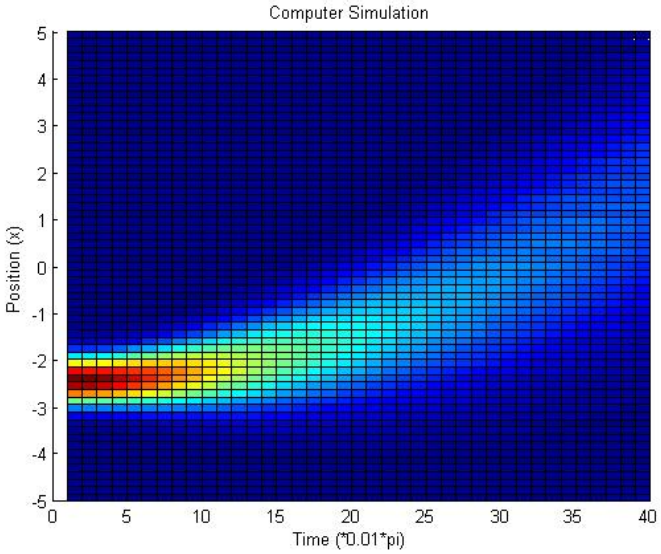

Figure 3.1: Gaussian of width 0.5 centered at -2.5 in a potential V = -5x. Number of qubits = 6. $\delta t = \frac{\pi}{100}$; x = -5 : 5

Chapter 4

Quantum Simulator

In this chapter we set out to simulate single particle Schrodinger equation using NMR.

4.1 Pseudo Pure States

NMR is an ensemble technique. So the task of preparing a pure state amounts to preparing all spin systems (roughly 10^{18} molecules) to the same state. This is almost impossible with NMR.

In equilibrium, the population distribution is Boltzmannian. The equilibrium density operator for an N-spin system is found to be

$$\rho_{eq} = \frac{1}{2^N}\left(\mathbb{I} + \frac{\hbar\gamma B_0}{kT}\sum_{j=1}^{N}\mathcal{I}_{jz}\right)^{1} \tag{4.1}$$

$$= \frac{1}{2^N}\left(\mathbb{I} + \epsilon\rho_{dev}\right) \tag{4.2}$$

where $\mathbb{I}$ represents an uniform background in the populations of the states. The probability (and hence NMR signal intensity) of a transition is proportional to the population difference between the two states involved. This implies that only the deviation part contributes to the NMR signal.

[1] Approximation at room temperatures where $\epsilon = \frac{\hbar\gamma B_0}{kT}$ is very low.

If we intend to create a pure state $|\psi\rangle$, then an ensemble, whose density matrix is

$$\rho \;=\; \frac{1}{2^N}(1-\epsilon)\mathbb{I} + \epsilon|\psi\rangle\langle\psi|, \tag{4.3}$$

mimics it fairly well. ϵ here is in the order of 10^{-5}.

Observe that the uniform background does not evolve under unitary transformations, as $U\mathbb{I}U^\dagger = \mathbb{I}$. Barring measurement all our operations are unitary. So ρ is a good enough pure state for our experiment.

4.1.1 Preparation

We prepare pseudo pure states for this experiment using *pairs of pseudopure states* (POPS)[17] technique. Difference between the equilibrium absorption spectrum and a selectively inverted absorption spectrum of an ancilla qubit gives the desired pseudopure state. As an illustration, consider a 3-qubit system. On taking the first qubit to be our ancilla, we have two computational qubits. To prepare $|10\rangle$ pseudo-pure state, we apply a transition selective pulse to invert the populations of $|010\rangle$ and $|110\rangle$. On taking difference between the two distributions, we have effectively equalised the populations of all states except that between $|010\rangle$ and $|110\rangle$, thereby killing all transitions other than $|010\rangle \leftrightarrow |110\rangle$. Please refer figure 4.1.1.

4.2 Evolution

We use GRAPE algorithm to generate pulses for all the four unitary operators mentioned in 3.3. Other than QFT and its inverse, the rest are implemented using simple phase gates. The conventional QFT which is given by

$$\widetilde{\psi} = \frac{1}{\sqrt{2\pi}}\Sigma_{n=0}^{N-1}\psi e^{\frac{2\pi i}{N}mn}\Delta x \tag{4.4}$$

is slightly different from the one we use (3.7) and has a circuit given in 4.2. Clearly this is no easy operation to implement as it has $\frac{n(n+1)}{2}$ gates - n are Hadamard gates and the rest are phase gates.

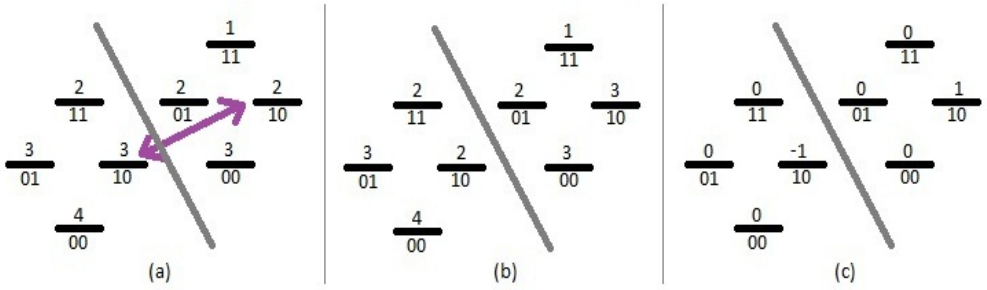

Figure 4.1: **Population distribution of spin states with respect to ancilla qubit.** (a) At thermal equilibrium. (b) On selective inversion of $|10\rangle$. (c) Difference between (a) and (b).

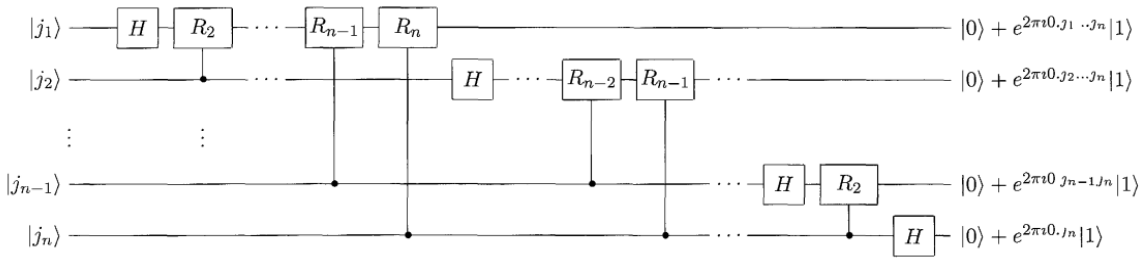

Figure 4.2:

We then design pulse sequences to be run on both equilibrium state and selectively inverted initial state, which are essentially the same except for the transition selective inversion.

The pulse sequences are given in 4.2. $\frac{\pi}{2}_x$ in the figure represents detection pulse. The boxed part in the figure is repeated in the sequence as many times as required. The gradient pulses are used to kill coherences (off-diagonal terms in the density matrix) as we are only interested in the population terms (diagonal terms). A gradient pulse creates an inhomogeneous magnetic field along the z-axis which make nuclei in different z-domains of the sample precess with different larmour frequencies. Coherences dephase in an inhomogeneous magnetic field.

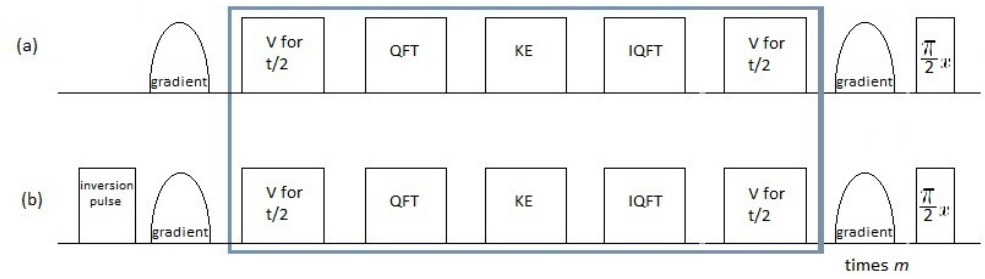

Figure 4.3: **Pulse sequence** (a) that evolves the equilibrium state (b) that performs selective inversion and evolves the ensuing state. *Difference between the end spectra gives the desired result.*

In a n-qubit system, we get n sets of 2^{n-1} resolved spectral lines of equal intensities. For this experiment, we take one of the qubits to be our ancilla. Therefore we have 2^{n-1} lines representing computational basis states. We evolve the two subspaces corresponding to the state of the first qubit simultaneously with a same unitary operator U. Therefore, (refer figure 4.1.1(c)) with POPS technique, the density matrix values of the states in the two subspaces differ only in sign - figure 4.2

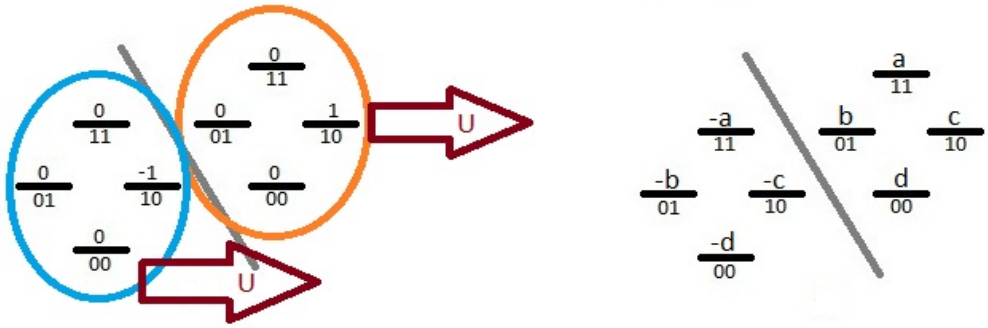

Figure 4.4:

The intensities of the spectral lines on the final spectrum give us the probability amplitudes of the evolved ψ.

Chapter 5

Results

5.1 System

We used 1-bromo-2,4,5-trifluorobenzene (BTFBz) in N-(4-methoxybenzylidene)-4-n-butylaniline (MBBA) - liquid crystal solvent for the experiment. It has three spin-$\frac{1}{2}$ ^{19}F nuclei and two spin-$\frac{1}{2}$ ^{1}H nuclei as shown in figure 5.1. Sample preparation involved adding $700\mu L$ of MBBA to $8\mu L$ of BTFBz in a NMR tube. The sample is repeatedly heated and mixed for homogenization, before loading the sample in the spectrometer.

The chemical shift and J-coupling values of the sample were about:

Chemical Shift	J-coupling	
v(1) = 6029	J(1,2) = 277	J(2,4) = 106
v(2) = -3680	J(1,3) = 116	J(2,5) = 1270
v(3) = -6743;	J(1,4) = 54	J(3,4) = 1532
v(4) = 50;	J(1,5) = 1556	J(3,5) = 55
v(5) = 29;	J(2,3) = -26	J(4,5) = -7.6

Our system thus has 5-qubits. Taking one of the qubits to be ancilla, we have a 4-qubit computational basis. The absorption spectrum of one of the ^{19}F nuclei (ancilla qubit) is shown in figure 5.2.

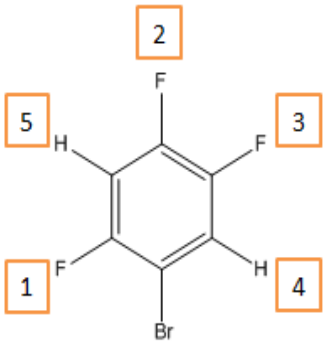

Figure 5.1: *Structure of BTFBz, which was used as a 5-qubit system for the simulation. Qubits are labelled.*

5.1.1 Labelling of Transitions

In a coupled n-spin system, each transition of i-th spin can be labelled using (n-1) bits, where each bit is either 0 or 1 corresponding to the state of the respective spin. The labelling however must be consistent with the connectivity of the transitions. The method we use to label the transitions is called *transition-tickling* technique which is explained in the appendix B.1.

Labelling done so for our system is depicted in figure 5.2 where the strings of bits are represented in decimal format.

5.2 Simulations

We tried simulating a variety of potentials as listed below. Parameters defining an experiment are

δt – Evolution period of ψ in every iteration

x – Domain of ψ which is divided into 2^n parts where n is the number of qubits.

V – Potential defined over x

ψ_0 – Initial wavefunction

Computer simulations with unitary matrices computed by GRAPE algorithm are also given below alongside corresponding the experimental NMR results.

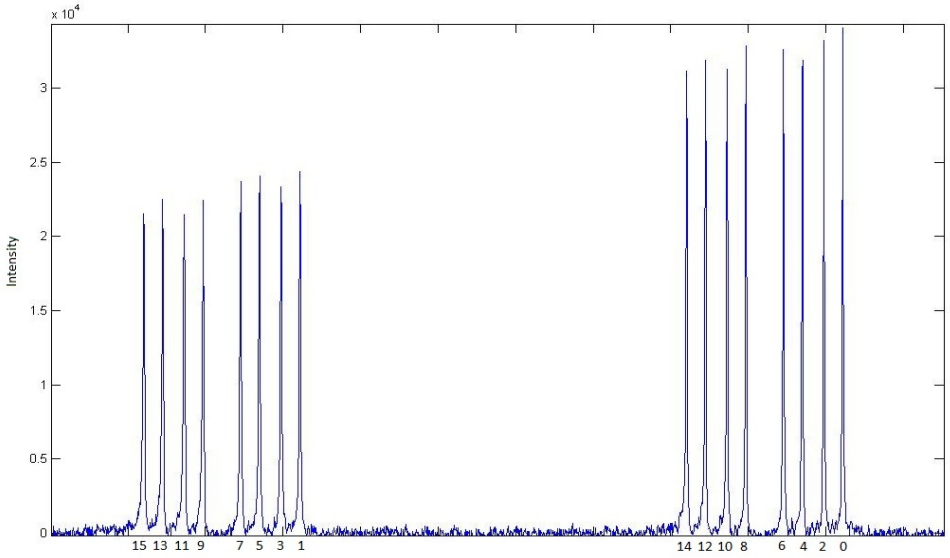

Figure 5.2:

5.2.1 Delta wavepacket in zero potential

$\delta t = \frac{\pi}{20}$; $x = -4 : 4$; $V = 0$; $|\psi_0\rangle = |8\rangle$. Results are shown in figure 5.3.

5.2.2 Bar Potential

$\delta t = \frac{\pi}{100}$; $x = -2 : 2$; $V = 100$ at 9 and 10 and zero elsewhere . $|\psi_0\rangle = |7\rangle$. Results are shown in figure 5.4.

5.2.3 Linear Potential

$\delta t = \frac{\pi}{20}$; $x = -4 : 4$; $V = -6x$. $|\rho_0\rangle = \frac{1}{8}|7\rangle\langle 7| + \frac{6}{8}|8\rangle\langle 8| + \frac{1}{8}|9\rangle\langle 9|$ Results are shown in figure 5.5.

5.2.4 Square-well Potential

$\delta t = \frac{\pi}{100}$; $x = -2 : 2$; $V = 0$ at 6,7 and 8 and +60 elsewhere . $|\psi_0\rangle = |7\rangle$. Results are shown in figure 5.6.

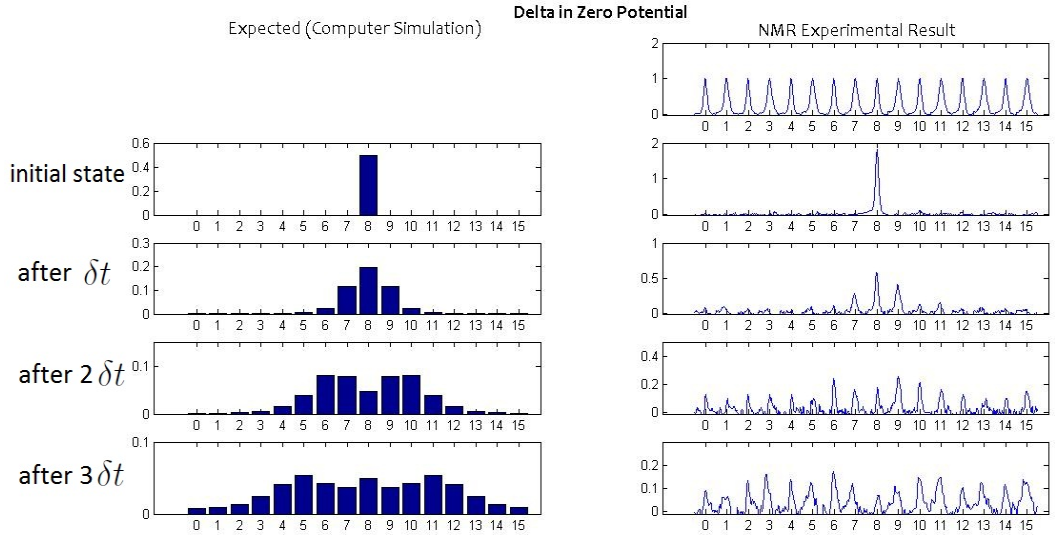

Figure 5.3: Free Particle

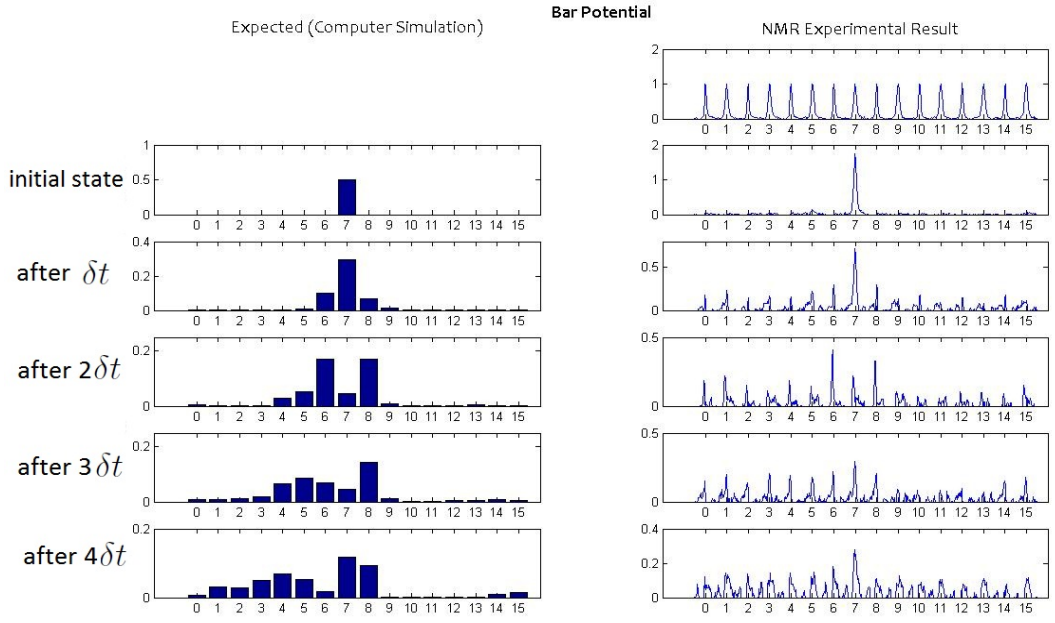

Figure 5.4: Bar Potential

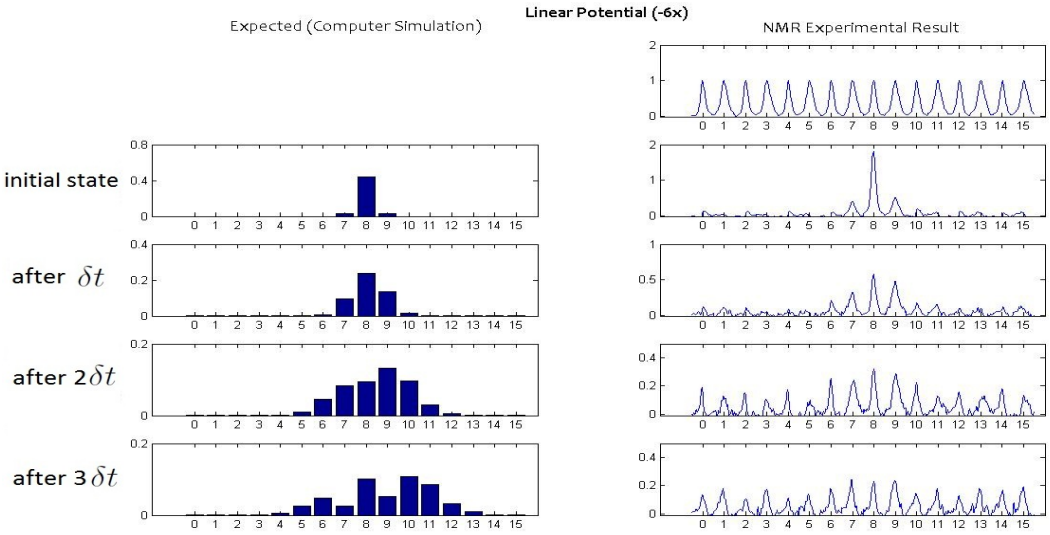

Figure 5.5: Linear Potential

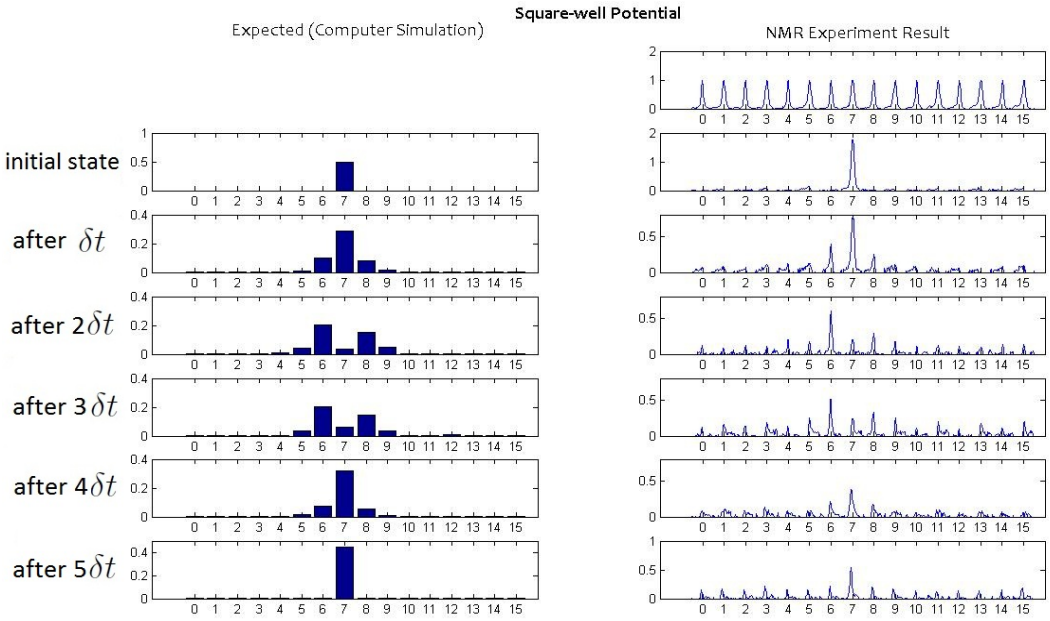

Figure 5.6: Square-well Potential

Chapter 6

Discussion

Though in theory, any potential can be simulated using the method described, in practice it is difficult to do so. This is because the GRAPE algorithm takes longer time to converge to a pulse sequence with increasing complexity of the target operator. Any potential more complex than quadratic will require decomposition of the target operator into simpler components in Pauli basis and rerunning GRAPE algorithm with clubbed converged components as initial guess. This is expected to reduce convergence time significantly.

We use liquid crystal medium (MBBA) rather than liquid medium for stronger J-couplings, which make gate implementation more efficient. As a trade off, we are let to deal with ever shifting spectra. This is because the coupling values are dependent on the orientation of the molecules to a good deal in a liquid crystal medium. The shift is non-linear and as our procedure involves taking a difference between two spectra for the final ensemble measurement, liquid crystal medium makes our results error prone.

Methods involving coherence terms can also be used which would enable us to initialise any given ψ rather than only those whose density matrix can be described with only population terms.

NMR is highly sensitive to ground vibrations. Care must be taken perform experiments in peaceful atmosphere. The construction work going around in Innovation Park, with all the hammering and banging, has ru-

ined our shim[1] parameters many a time.

The use of POPS technique along with shifting spectra makes the results error prone. Solutions to minimise this error with better sample selection or technique is sought. For a more efficient method, one can also tweak the GRAPE algorithm or just come up with a more efficient code for the existing GRAPE algorithm that which converges to a desired pulse sequence faster.

[1]Shimming is done to correct for inhomogeneities in the external magnetic field

References

[1] G. Moore, Cramming more components onto integrated circuits, Electronics 38 (1965) 8.

[2] R. Feynman, Simulating physics with computers, Int. J. Theor. Phys. 21 (1982) 467.

[3] P. W. Shor, Polynomial-time algorithms for prime factorization and discrete algorithms on quantum computer, SIAM Rev 41 (1999) 303.

[4] L. K. Grover, Quantum mechanics helps in searching for a needle in a haystack, Phys. Rev. Lett. 79 (1997) 325.

[5] C. H. Bennett, G. Brassard, C. CrÃĽpeau, R. Jozsa, A. Peres, W. K. Wootters , Teleporting an unknown quantum state via dual classical and einstein-podolsky-rosen channels, Phys. Rev. Lett. 70 (1993) 1895.

[6] D. Deutsch, Quantum theory, the church-turing principle and the universal quantum computer, Proc. R. Soc. London A 400 (1985) 97.

[7] J. A. Jones, Nmr quantum computation: a critical evaluation, Fort. der Physik 48 (2000) 909.

[8] J. A. Jones, M. Mosca, Implementation of a quantum algorithm on a nuclear magnetic resonance quantum computer, J. Chem. Phys. 109 (1998) 1648.

[9] J. A. Jones, M. Mosca, R. H. Hansen, Implementation of a quantum search algorithm on a quantum computer, Nature 393 (1998) 344.

[10] J. A. Jones, M. Mosca, Approximate quantum counting on an nmr ensemble quantum computer, Phys. Rev. Lett. 83 (1999) 1050–1053.

[11] S. L. Braunstein, C. M. Caves, R. Jozsa, N. Linden, S. Popescu, R. Schack, Separability of very noisy mixed states and implications for nmr quantum computing', journal =.

[12] Navin Khaneja, Timo Reiss, Cindie Kehlet, Thomas Schulte-Herbruggen, Steffen J. Glaser, Optimal control of coupled spin dynamics: design of nmr pulse sequences by gradient ascent algorithms, Journal of Magnetic Resonance 172 (2005) 296–305.

[13] M. Born, Quantenmechanik der stoÃ§vorgÂÍange, Z. Phys. 38 (1926) 803.

[14] D. K. Park, O. Moussa, R. Laflamme , Three path interference using nuclear magnetic resonance: a test of the consistency of born's rule, New J. Phys. 14 (2012) 113025.

[15] Hans De Raedt, K. Michielsen, k. Hess, Analysis of multipath interference in three-slit experiments, Phys. Rev. A 85 (2012) 012101.

[16] G. Benenti, G. Strini, Quantum simulation of the single-particle schrÃűdinger equation, AJP 76 (2008) 657.

[17] B. M. Fung, Use of pairs of psedopure states for NMR quantum computing, Phys. Rev. A 63 (2001) 022304.

Appendix A

Long Proofs

A.1 Discrete Fourier Transform Sec.

$$\widehat{\psi} = \frac{1}{\sqrt{2\pi}} \int_a^b \psi e^{-ikx} dx$$
$$\longrightarrow \widehat{\psi} = \frac{1}{\sqrt{2\pi}} \Sigma_{n=0}^{N-1} \psi e^{-ikx} \Delta x$$

Consider e^{-ikx}:
Substituting

$$k_m = k_0 + m\Delta k$$
$$x_n = x_0 + n\Delta x$$

into the expression for e^{-ikx}

$$\begin{aligned} e^{-ikx} &= e^{-i(k_0+\Delta km)x_0} e^{-ik_0\Delta xn} e^{-i\Delta km\Delta xn} \\ &= e^{-i(k_0+\Delta km)x_0} e^{-ik_0\Delta xn} e^{-\frac{2\pi i}{N}mn} \\ &= e^{-i(k_0+\Delta km)x_0} e^{i\pi n} e^{-\frac{2\pi i}{N}mn} \qquad (k_0 = \frac{-\pi}{\Delta x}) \end{aligned} \tag{A.1}$$

Here x_0 can be chosen to be 0 as the domain of x is arbitrary thus far. So we can safely ignore the first exponential.

$$e^{-ikx} = e^{i\pi n} e^{\frac{-2\pi i}{N} mn}$$

This implies,

$$\widehat{\psi} = \frac{1}{\sqrt{2\pi}} \Sigma_{n=0}^{N-1} \psi e^{i\pi n} e^{\frac{-2\pi i}{N} mn} \Delta x$$

A.2 Trotter decomposition

Consider

$$e^{i\frac{At}{n}} = \mathbb{I} + \frac{1}{n} iAt + O\left(\frac{1}{n^2}\right)$$

Thus

$$e^{i\frac{At}{n}} e^{i\frac{Bt}{n}} = \mathbb{I} + \frac{1}{n} i(A+B)t + O\left(\frac{1}{n^2}\right)$$

Taking products of n such terms,

$$(e^{i\frac{At}{n}} e^{i\frac{Bt}{n}})^n = \mathbb{I} + \sum_{k=1}^{n} \binom{n}{k} \frac{1}{n^k} [i(A+B)t]^k + O\left(\frac{1}{n}\right) \tag{A.2}$$

Also,

$$\binom{n}{k} \frac{1}{n^k} = \left(1 + O(\frac{1}{n})\right) \frac{1}{k!}$$

which makes A.2, on application of lim $n \to \infty$

$$\begin{aligned} \lim_{n\to\infty} (e^{i\frac{At}{n}} e^{i\frac{Bt}{n}})^n &= \lim_{n\to\infty} \left(\sum_{k=0}^{n} \frac{[i(A+B)t]^k}{k!} \left(1 + O(\frac{1}{n})\right) \right) + O\left(\frac{1}{n}\right) \\ &= e^{i(A+B)t} \end{aligned}$$

Please note, that nowhere has it been assumed anything about the commutation between A and B. Similarly,

$$e^{i(A+B)\Delta t} = e^{i\frac{A\Delta t}{2}} e^{iB\Delta t} e^{i\frac{A\Delta t}{2}} + O\left(\Delta t^3\right)$$

Appendix B

Detailed Explanations

B.1 Transition Labelling using Tickling Experiment

A n-spin system has a total of $n \times 2^{n-1}$ transitions. Two transitions that share a common energy level are said to be *connected*. The technique involves inverting one transition (using a π pulse) while the other transition is either suppressed (regressive connectivity) or enhanced (progressive connectivity) (Please refer figure B.1). The first transition is labelled arbitrarily and progressive and regressive connections are made for every transition, with the help of which we can consistently label the transitions.

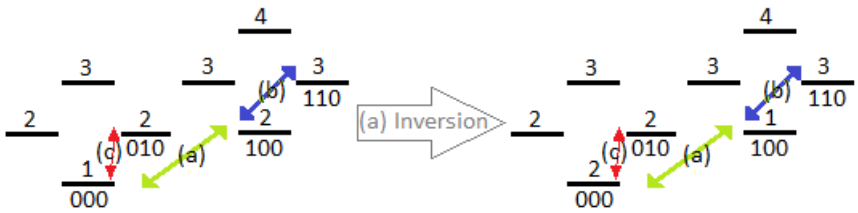

Figure B.1: Transitions (a) and (b) and (a) and (c) are separately connected. Inverting (a) enhances (b) and suppresses (c)